J|A|C|S
ARTICLES
Published on Web 06/18/2003

Reductive Elimination/Oxidative Addition of Carbon−Hydrogen Bonds at Pt(IV)/Pt(II) Centers: Mechanistic Studies of the Solution Thermolyses of $Tp^{Me_2}Pt(CH_3)_2H$

Michael P. Jensen,[‡] Douglas D. Wick,[‡] Stefan Reinartz,[§] Peter S. White,[§] Joseph L. Templeton,*[,§] and Karen I. Goldberg*[,‡]

Contribution from the Department of Chemistry, Box 351700, University of Washington, Seattle, Washington 98195-1700, and the Department of Chemistry, University of North Carolina, Chapel Hill, North Carolina 27599-3290

Received September 9, 2002; E-mail: goldberg@chem.washington.edu, joetemp@unc.edu

Abstract: Reductive elimination of methane occurs upon solution thermolysis of κ^3-$Tp^{Me_2}Pt^{IV}(CH_3)_2H$ (**1**, Tp^{Me_2} = hydridotris(3,5-dimethylpyrazolyl)borate). The platinum product of this reaction is determined by the solvent. C−D bond activation occurs after methane elimination in benzene-d_6, to yield κ^3-$Tp^{Me_2}Pt^{IV}(CH_3)(C_6D_5)D$ (**2-*d*$_6$**), which undergoes a second reductive elimination/oxidative addition reaction to yield isotopically labeled methane and κ^3-$Tp^{Me_2}Pt^{IV}(C_6D_5)_2D$ (**3-*d*$_{11}$**). In contrast, κ^2-$Tp^{Me_2}Pt^{II}(CH_3)(NCCD_3)$ (**4**) was obtained in the presence of acetonitrile-d_3, after elimination of methane from **1**. Reductive elimination of methane from these Pt(IV) complexes follows first-order kinetics, and the observed reaction rates are nearly independent of solvent. Virtually identical activation parameters ($\Delta H^{\ddagger}_{obs} = 35.0 \pm 1.1$ kcal/mol, $\Delta S^{\ddagger}_{obs} = 13 \pm 3$ eu) were measured for the reductive elimination of methane from **1** in both benzene-d_6 and toluene-d_8. A lower energy process ($\Delta H^{\ddagger}_{scr} = 26 \pm 1$ kcal/mol, $\Delta S^{\ddagger}_{scr} = 1 \pm 4$ eu) scrambles hydrogen atoms of **1** between the methyl and hydride positions, as confirmed by monitoring the equilibration of κ^3-$Tp^{Me_2}Pt^{IV}(CH_3)_2D$ (**1-*d*$_1$**) with its scrambled isotopomer, κ^3-$Tp^{Me_2}Pt^{IV}(CH_3)(CH_2D)H$ (**1-*d*$_1$′**). The σ-methane complex κ^2-$Tp^{Me_2}Pt^{II}(CH_3)(CH_4)$ is proposed as a common intermediate in both the scrambling and reductive elimination processes. Kinetic results are consistent with rate-determining dissociative loss of methane from this intermediate to produce the coordinatively unsaturated intermediate [$Tp^{Me_2}Pt^{II}(CH_3)$], which reacts rapidly with solvent. The difference in activation enthalpies for the H/D scrambling and C−H reductive elimination provides a lower limit for the binding enthalpy of methane to [$Tp^{Me_2}Pt^{II}(CH_3)$] of 9 ± 2 kcal/mol.

Introduction

Exploitation of the vast reserves of alkanes as chemical feedstocks will require the development of methodology for the selective functionalization of saturated hydrocarbon C−H bonds. Alkane C−H bonds are difficult to activate selectively, a result of their instrincally high bond strength and low acidity, combined with a strong thermodynamic proclivity toward overoxidation.

Despite intensive investigations of several natural and artificial systems that activate such bonds, the development of a significant industrial process remains elusive.[1−3] One promising approach to solving this problem takes advantage of the selectivity of C−H activation reactions of low-valent, low-coordinate complexes of the late transition metals. Thirty years ago, Shilov reported the selective oxidation of methane to methanol and methyl chloride by Pt(II) and Pt(IV) chloride salts in aqueous solution.[2] Although a Pt(II) species is the catalyst in this reaction, consumption of Pt(IV) as a stoichiometric oxidant makes the system impractical. More recently, Periana et al. used a discrete (bipyrimidine)Pt(II) complex in sulfuric acid with SO_3 as the oxidant to convert methane to methyl bisulfate.[4] Further advances have shown the potential of H_2O_2 and O_2 as oxidants in platinum(II)-catalyzed alkane oxidation reactions.[5]

The first step in platinum(II)-catalyzed alkane oxidation reactions is the activation of a C−H bond, resulting in formation of a Pt(II) alkyl. This occurs either via oxidative addition followed by deprotonation of the resulting Pt(IV) alkyl hydride or by direct deprotonation of a Pt(II) σ-alkane complex.[6] Evidence obtained primarily from protonation studies of model

[‡] University of Washington.
[§] University of North Carolina.

(1) Recent reviews: (a) Shilov, A. E.; Shul'pin, G. B. *Chem. Rev.* **1997**, *97*, 2879. (b) Jones, W. D. *Top. Organomet. Chem.* **1999**, *3*, 9. (c) Sen, A. *Top. Organomet. Chem.* **1999**, *3*, 80. (d) Crabtree, R. H. *J. Chem. Soc., Dalton Trans.* **2001**, 2437. (e) Labinger, J. A.; Bercaw, J. E. *Nature* **2002**, 417, 507.
(2) (a) Shilov, A. E. *Activation of Saturated Hydrocarbons by Transition Metal Complexes*; D. Riedel: Dordrecht, The Netherlands, 1984. (b) Shilov, A. E.; Shul'pin, G. B. *Activation and Catalytic Reactions of Saturated Hydrocarbons in the Presence of Metal Complexes*; Kluwer: Boston, 2000.
(3) Arndtsen, B. A.; Bergman, R. G.; Mobley, T. A.; Peterson, T. H. *Acc. Chem. Res.* **1995**, *28*, 154.
(4) Periana, R. A.; Taube, D. J.; Gamble, S.; Taube, H.; Satoh, T.; Fujii, H. *Science* **1998**, *280*, 560.
(5) (a) Thorn, D. L.; Roe, D. C.; DeVries, N. *J. Mol. Catal. A* **2002**, *189*, 17. (b) Lin, M.; Shen, C.; Garcia-Zayas, E. A.; Sen, A. *J. Am. Chem. Soc.* **2001**, *123*, 1000.
(6) Stahl, S. S.; Labinger, J. A.; Bercaw, J. E. *Angew. Chem., Int. Ed.* **1998**, *37*, 2180, and references therein.

10.1021/ja028477t CCC: $25.00

Scheme 1

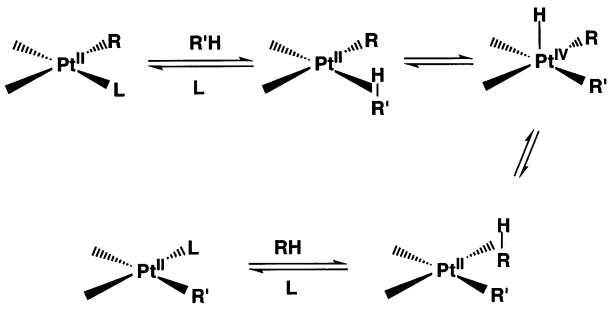

Pt(II) alkyl complexes supports the oxidative addition pathway.[6,7] A number of C−H activation reactions at Pt(II) characterized by alkyl/aryl exchange with hydrocarbon solvents have been documented, but since the proposed bis(hydrocarbyl) Pt(IV) hydride oxidative addition intermediates were not observed, the involvement of Pt(IV) could not be unambiguously established.[8−10]

A common feature of Pt(II) complexes that activate C−H bonds is the presence of a good leaving group (triflate, perfluoropyridine, water, trifluoroethanol, etc.) in the square-planar Pt(II) coordination sphere. Replacement of this ligand (L) with a hydrocarbon forms the Pt(II) σ-alkane complex, thought to be the first intermediate in the C−H activation reaction (Scheme 1).[6] While convincing evidence has been presented for an associative displacement of the ligand L by the alkane in one type of ligand system,[8b,11] the mechanism of this exchange reaction likely depends on the specific ligand set and charge on the metal center (see Discussion section). Facile C−H bond cleavage occurs from the σ-alkane intermediate via either σ-bond metathesis or oxidative addition. The oxidative addition pathway is shown in Scheme 1 and would produce a five-coordinate bis(hydrocarbyl) hydride Pt(IV) intermediate. Reversal of the reaction sequence but involving the original hydrocarbyl ligand completes the exchange. Detailed mechanistic studies of these C−H bond activation reactions have been hampered by the elusive nature of the five-coordinate Pt(IV) alkyl hydride species. Five-coordinate Pt(IV) alkyls have been consistently proposed as intermediates in oxidative addition/reductive elimination reactions at Pt(II)/Pt(IV) involving C−H, C−C, and C−X bonds,[12−17] and recently, the first examples of five-coordinate Pt(IV) complexes, namely, the trimethyl complex (nacnac)$Pt^{IV}Me_3$ (nacnac$^-$ = [{(*o*-^{i}Pr$_2$C$_6$H$_3$)NC(CH$_3$)}$_2$CH]$^-$)[18] and the silyl dihydride complex [κ^2-((Hpz^{Me_2})BH(pz^{Me_2})$_2$)Pt(H)$_2$(SiEt$_3$)][BAr′$_4$] (BAr′$_4$ = B(C$_6$H$_3$(CF$_3$)$_2$)$_4$),[19] have been isolated and structurally characterized.[20] Structurally analogous five-coordinate Pt(IV) alkyl hydrides are expected to undergo facile reductive elimination.

The first examples of C−H oxidative addition reactions to Pt(II) to yield stable *six-coordinate* Pt(IV) alkyl hydrides were reported in 1997 (Scheme 2).[21] Reaction of K[κ^2-$Tp^{Me_2}Pt^{II}$(CH$_3$)$_2$] (Tp^{Me_2} = hydridotris(3,5-dimethylpyrazolyl)borate) with B(C$_6$F$_5$)$_3$ in hydrocarbon solvent (R−H) produces the Pt(IV) di(hydrocarbyl) hydride species κ^3-$Tp^{Me_2}Pt^{IV}$(CH$_3$)(R)(H) (R = phenyl, cyclohexyl, pentyl). Abstraction of a methide group from the starting Pt(II) anion was proposed to generate the key three-coordinate species [κ^2-$Tp^{Me_2}Pt^{II}$(CH$_3$)], which reacts with hydrocarbons. Oxidative addition of the C−H bond produces the five-coordinate Pt(IV) hydrocarbyl hydride, which is rapidly trapped by coordination of the third arm of the Tp^{Me_2} ligand to yield a stable six-coordinate Pt(IV) complex (Scheme 2). A similar proposal of C−H bond activation by a four-coordinate κ^2-Tp^{Me_2} Rh(I) σ-alkane species followed by attachment of the third pyrazolyl to the Rh(III) alkyl hydride product was supported by ultrafast time-resolved infrared experiments.[22]

The surprising stability of the Pt(IV) dialkyl hydrides κ^3-$Tp^{Me_2}Pt^{IV}$(CH$_3$)(R)(H) has been attributed to the chelating ability of the tridentate ligand, which inhibits formation of a five-coordinate intermediate from which reductive elimination is expected to take place.[23] Other examples of unusually stable Pt(IV) alkyl hydrides also contain ligands that do not easily dissociate from the metal center.[12b−d,17,24]

Direct examination of the mechanism of C−H bond activation that occurs upon reaction of K[κ^2-$Tp^{Me_2}Pt^{II}Me_2$] with B(C$_6$F$_5$)$_3$ in hydrocarbon solvent was constrained by the requisite bimolecular activation step with B(C$_6$F$_5$)$_3$ and the presence of competing reactions. We now report that this C−H activation can be successfully studied via investigation of the microscopic reverse reaction, C−H reductive elimination from the known compound κ^3-$Tp^{Me_2}Pt^{IV}$(CH$_3$)$_2$(H) (**1**).[23] At elevated temperature, C−H reductive elimination from **1** cleanly generates CH_4 and a Pt(II) species that can activate hydrocarbon C−H bonds. This

(7) Wik, B. J.; Lersch, M.; Tilset, M. *J. Am. Chem. Soc*. **2002**, *124*, 12116.
(8) (a) Zhong, H. A.; Labinger, J. A.; Bercaw, J. E. *J. Am. Chem. Soc*. **2002**, *124*, 1378. (b) Johansson, L.; Ryan, O. B.; Rømming, C.; Tilset, M. *J. Am. Chem. Soc*. **2001**, *123*, 6579. (c) Johansson, L.; Tilset, M.; Labinger, J. A.; Bercaw, J. E. *J. Am. Chem. Soc*. **2000**, *122*, 10846. (d) Heiberg, H.; Johansson, L.; Gropen, O.; Ryan, O. B.; Swang, O.; Tilset, M. *J. Am. Chem. Soc*. **2000**, *122*, 10831. (e) Johansson, L.; Ryan, O. B.; Tilset, M. *J. Am. Chem. Soc*. **1999**, *121*, 1974.
(9) (a) Holtcamp, M. W.; Henling, L. M.; Day, M. W.; Labinger, J. A.; Bercaw, J. E. *Inorg. Chim. Acta* **1998**, *270*, 467. (b) Holtcamp, M. W.; Labinger J. A.; Bercaw, J. E. *J. Am. Chem. Soc*. **1997**, *119*, 848.
(10) (a) Brainard, R. L.; Nutt, W. R.; Lee, T. R.; Whitesides, G. M. *Organometallics* **1988**, *7*, 2379. (b) Peters, R. G.; White, S.; Roddick, D. M. *Organometallics* **1998**, *17*, 4493.
(11) (a) Johansson, L.; Tilset, M. *J. Am. Chem. Soc*. **2001**, *123*, 739. (b) Procelewska, J.; Zahl, A.; van Eldik, R.; Zhong, H. A.; Labinger, J. A.; Bercaw, J. E. *Inorg. Chem*. **2002**, *41*, 2808.
(12) (a) Hill, G. S.; Rendina, L. M.; Puddephatt, R. J. *Organometallics* **1995**, *14*, 4966. (b) Jenkins, H. A.; Yap, G. P. A.; Puddephatt, R. J. *Organometallics* **1997**, *16*, 1946. (c) Fekl, U.; Zahl, A.; van Eldik, R. *Organometallics* **1999**, *18*, 4156. (d) Prokopchuk, E. M.; Puddephatt, R. J. *Organometallics* **2003**, *22*, 563. (e) Prokopchuk, E. M.; Puddephatt, R. J. *Organometallics* **2003**, *22*, 787.
(13) Stahl, S. S.; Labinger, J. A.; Bercaw, J. E. *J. Am. Chem. Soc*. **1996**, *118*, 5961.
(14) (a) Goldberg, K. I.; Yan, J. Y.; Breitung, E. M. *J. Am. Chem. Soc.* **1995**, *117*, 6889. (b) Williams, B. S.; Holland, A. W.; Goldberg, K. I. *J. Am. Chem. Soc.* **1999**, 121, 252. (c) Crumpton, D. M.; Goldberg, K. I. *J. Am. Chem. Soc.* **2000**, *122*, 962. (d) Williams, B. S.; Goldberg, K. I. *J. Am. Chem. Soc*. **2001**, *123*, 2576.
(15) (a) Brown, M. P.; Puddephatt, R. J.; Upton, C. E. E. *J. Chem. Soc., Dalton Trans*. **1974**, 2457. (b) Roy, S.; Puddephatt, R. J.; Scott, J. D. *J. Chem. Soc., Dalton Trans.* **1989**, 2121. (c) Hill, G. S.; Yap, G. P. A.; Puddephatt, R. J. *Organometallics* **1999**, *18*, 1408.
(16) Fekl, U.; Goldberg, K. I. *Adv. Inorg. Chem.* **2003**, 54, in press.
(17) Puddephatt, R. J. *Coord. Chem. Rev.* **2001**, *219*, 157.
(18) Fekl, U.; Kaminsky, W.; Goldberg, K. I. *J. Am. Chem. Soc*. **2001**, *123*, 6423.
(19) Reinartz, S.; White, P. S.; Brookhart, M.; Templeton, J. L. *J. Am. Chem. Soc.* **2001**, *123*, 6425.
(20) Puddephatt, R. J. *Angew Chem., Int. Ed*. **2002**, *41*, 261.
(21) Wick, D. D.; Goldberg, K. I. *J. Am. Chem. Soc*. **1997**, *119*, 10235.
(22) Bromberg, S. E.; Yang, H.; Asplund, M. C.; Lian, T.; McNamara, B. K.; Kotz, K. T.; Yeston, J. S.; Wilkens, M.; Frei, H.; Bergman, R. G.; Harris, C. B. *Science* **1997**, *278*, 260.
(23) O'Reilly, S. A.; White, P. S.; Templeton, J. L. *J. Am. Chem. Soc*. **1996**, *118*, 5684.
(24) (a) Canty, A. J.; Dedieu, A.; Jin, H.; Milet, A.; Richmond, M. K. *Organometallics* **1996**, *15*, 2845. (b) Hill, G. S.; Vittal, J. J.; Puddephatt, R. J. *Organometallics* **1997**, *16*, 1209. (c) Prokopchuk, E. M.; Jenkins, H. A.; Puddephatt, R. J. *Organometallics* **1999**, *18*, 2861. (d) Haskel, A.; Keinan, E. *Organometallics* **1999**, *18*, 4677. (e) Vedernikov, A. N.; Caulton, K. G. *Angew. Chem. Int Ed*. **2002**, *41*, 4102. (f) Vedernikov, A. N.; Caulton, K. G. *Chem. Commun*. **2003**, 358.

Scheme 2

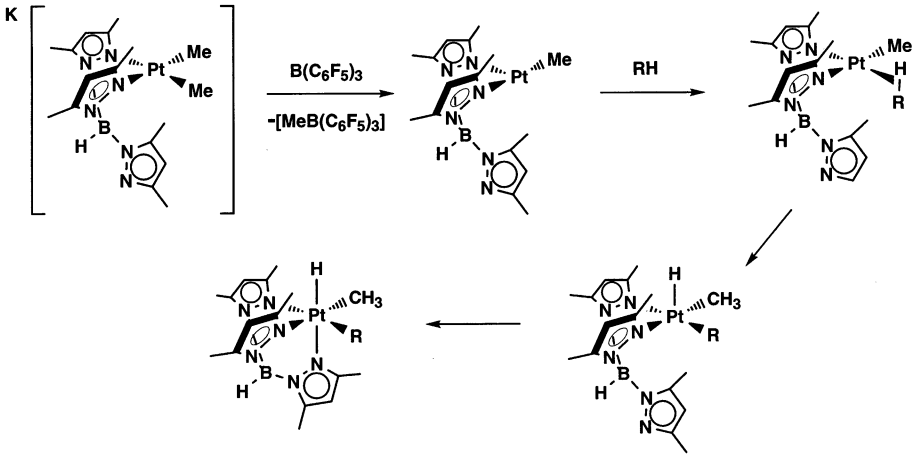

Scheme 3

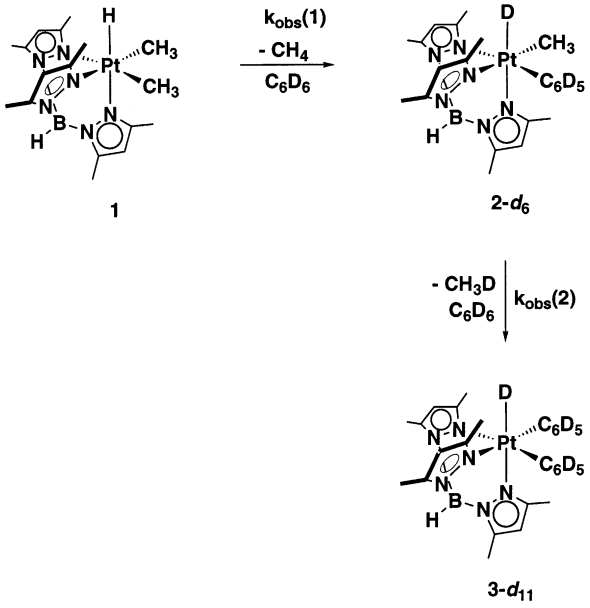

approach has accommodated detailed kinetic and mechanistic studies of the C−H bond cleavage/formation reaction. Our results are best explained by the involvement of a Pt(II) σ-alkane intermediate and a dissociative mechanism for the loss of alkane from this intermediate. The unsaturated [κ^2-$Tp^{Me_2}Pt^{II}(CH_3)$] fragment is strongly implicated in these C−H activation reactions. A minimum binding enthalpy of methane to the Pt(II) species [$Tp^{Me_2}Pt^{II}(CH_3)$] was also calculated.

Results

Thermolysis of $Tp^{Me_2}Pt^{IV}(CH_3)_2H$ (1) in C_6D_6. The Pt(IV) complex $Tp^{Me_2}Pt^{IV}(CH_3)_2H$ (**1**)[23] was heated in C_6D_6 at 110 °C, and the thermal reaction was monitored periodically at room temperature by ^{1}H NMR spectroscopy. Reductive elimination of methane (δ 0.15) was observed, and the reaction followed first-order kinetic behavior with respect to the disappearance of **1** (k_{obs}(**1**) = 6.73 × 10^{-5} s^{-1}, Table S1). The Pt(IV) methyl phenyl deuteride complex $Tp^{Me_2}Pt^{IV}(CH_3)(C_6D_5)(D)$ (**2-*d*$_6$**)[21] was generated by activation of the C_6D_6 solvent (Scheme 3). The initial Pt(IV) product **2-*d*$_6$** underwent further reaction under the thermolysis conditions to eliminate methane-d_1 (with some methane-d_2, see below) and form the Pt(IV) diphenyl deuteride

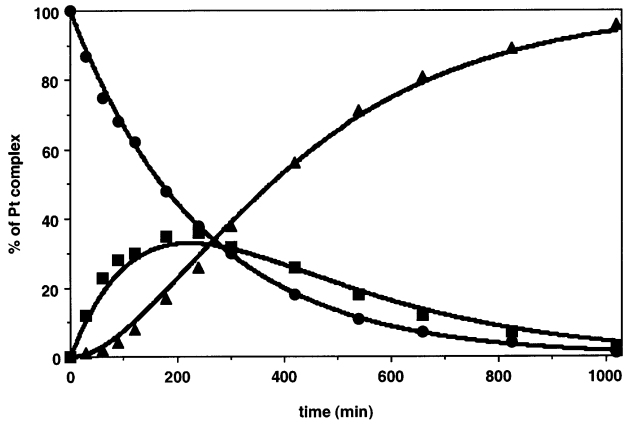

Figure 1. Distribution of species vs time for the thermolysis of **1** in C_6D_6 at 110 °C (● = **1**, ■ = **2-*d*$_6$**, ▲ = **3-*d*$_{11}$**).

complex $Tp^{Me_2}Pt^{IV}(C_6D_5)_2(D)$[23] (**3-*d*$_{11}$**) (Scheme 3). The course of this reaction sequence—the disappearance of **1**, the appearance and disappearance of **2-*d*$_6$**, and the appearance of **3-*d*$_{11}$**—was easily monitored via the Tp^{Me_2} methine region in the ^{1}H NMR spectrum. Monitoring the relative intensities of each set of methine signals against the combined total over time yielded kinetic data that were fit to the known solution of differential equations for consecutive, irreversible first-order reactions,[25] Figure 1.

Despite the apparent simplicity of this chemistry, several complications warrant comment. First, the kinetic fits gave a small but reproducible systematic deviation for the concentrations of **2-*d*$_6$** and **3-*d*$_{11}$**. Note that the fit as shown in Figure 1 slightly overestimates the accumulation of the final product **3-*d*$_{11}$** at early reaction times and then slightly underestimates the concentration of **3-*d*$_{11}$** toward the end. Similarly, the parameters underestimate the concentration of **2-*d*$_6$** at early reaction times and overestimate it at later times. Such errors would result if rate constant k_{obs}(**2**) (Scheme 3) increased with time. In addition, monitoring evolved methane isotopomers by ^{1}H NMR indicated that CH_4 accumulated immediately, followed by CH_3D after the expected induction period (Scheme 3). However, CH_2D_2 also appeared after a longer induction. Furthermore, isotopomers of **2-*d*$_6$** and **3-*d*$_{10}$** with protons in the hydride position as well

(25) Espenson, J. H. *Chemical Kinetics and Reaction Mechanisms*, 2nd ed.; McGraw-Hill: New York, 1995; p 71.

Scheme 4

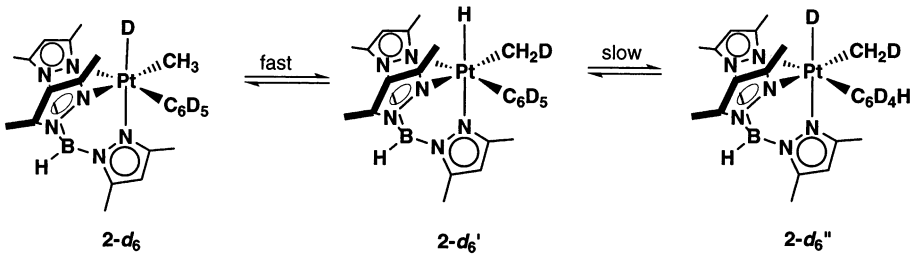

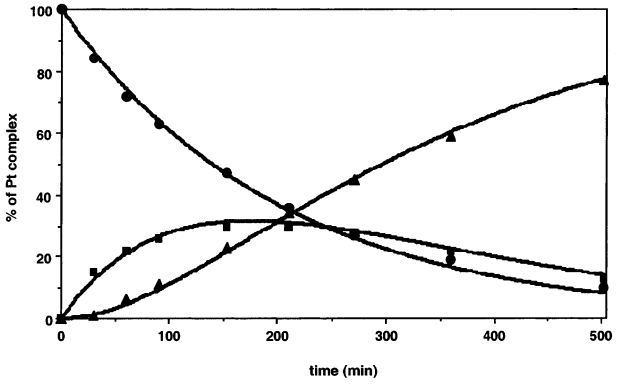

Figure 2. Distribution of species vs time for the thermolysis of **1**-d_7 in C_6D_6 at 110 °C (● = **1**-d_7, ■ = **2**-d_9, ▲ = **3**- d_{11}).

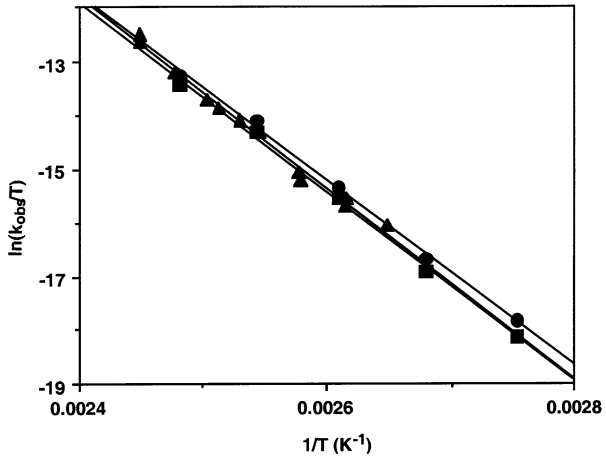

Figure 3. Eyring plot for the thermolysis of **1** in benzene-d_6 and toluene-d_8. Kinetic data are plotted for methane elimination reactions, from **1** (■) and from **2**-d_6 (●) in benzene-d_6, and from **1** in toluene-d_8 (▲).

as the phenyl ring positions were observed by ^{1}H NMR spectroscopy.

These observations are consistent with a relatively fast exchange of hydrogen atoms between the hydride and methyl positions, coupled with a slow exchange of hydride and phenyl positions in the intermediate species **2**-d_6 (Scheme 4). In this way, another deuteron can leak into the second reductive elimination of methane (second reaction in Scheme 3), producing CH_2D_2 and perturbing the observed rate constant through a weighted sum of k_H and k_D, which continuously increases in magnitude. Fortunately, the kinetic effect is small (<5%) and a reasonable estimate of an average value of k_{obs}(**2**) = 8.3 × 10^{-5} s^{-1} at 110 °C can be obtained over the course of the second elimination (Figure 1, Table S1).

An inverse kinetic isotope effect for the methane reductive elimination was confirmed by investigating the rate of CD_4 reductive elimination from $Tp^{Me_2}Pt^{IV}(CD_3)_2D$ (**1**-d_7). The kinetic fit for reductive elimination from **1**-d_7 is shown in Figure 2. The improved fit for the second reductive elimination reaction is consistent with the fact that isotopic scrambling is not possible in the perdeuterated system. The rate constants for the two eliminations, k_{obs}(1) and k_{obs}(2) (Scheme 3), calculated from the kinetic fits are listed in Table S1 for both **1** and **1**-d_7. An inverse isotope effect of k_H/k_D = 0.81 ± 0.03 was calculated for the first methane reductive elimination, and a similar $k_H/k_D \leq 0.78$ ± 0.03 was found for the second elimination.

The thermolysis reaction of **1** in C_6D_6 was carried out at temperatures between 90.0 and 130.0 °C, and nearly identical activation parameters were found for both eliminations from the Eyring plots, Figure 3; $\Delta H^{\ddagger}_{obs}(1)$ = 35.0 ± 1.1 kcal/mol and $\Delta S^{\ddagger}_{obs}(1)$ = 13 ± 3 eu for the first methane reductive elimination and $\Delta H^{\ddagger}_{obs}(2)$ = 34.0 ± 1.0 kcal/mol and $\Delta S^{\ddagger}_{obs}$-(2) = 11 ± 3 eu for the second elimination.

The final perdeutero diphenyl deuteride Pt(IV) product **3**-d_{11} was stable to prolonged thermolysis. After ca. 30 h at 110.0 °C,

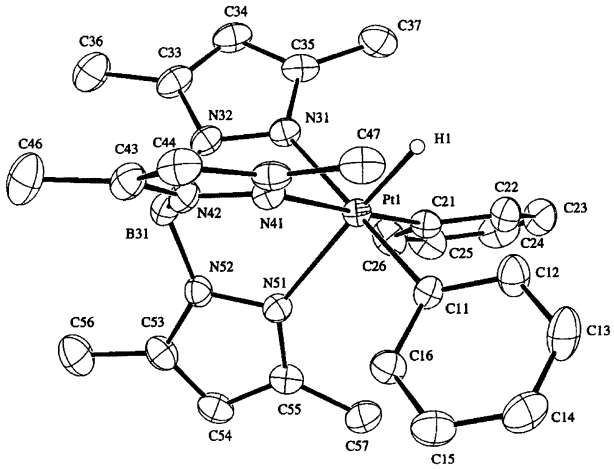

Figure 4. ORTEP diagram of κ^3-$Tp^{Me_2}Pt(Ph)_2H$ (**3**). Ellipsoids are drawn with 50% probability.

no growth of the C_6D_5H residual solvent resonance was observed. This is consistent with an earlier report that Tp^{Me_2}-$Pt(Ph)_2H$ (**3**) is stable in refluxing toluene for at least a period of 15 h.[23] The diphenyl hydride complex **3** has also been characterized by X-ray crystallography. An ORTEP diagram is shown in Figure 4, with bond lengths and bond angles for the diphenyl hydride complex κ^3-$Tp^{Me_2}Pt(Ph)_2H$ (**3**) listed in Table 1. The geometry is octahedral with the angle between the two phenyl ligands opened to 95°. The corresponding C−Pt−C angle in the dimethyl hydride complex is 90°.[23] The trans influence of the hydride ligand is reflected in the long Pt−N bond distance of 2.183(3) Å compared to Pt−N distances of 2.145(3) and 2.149(3) Å for the nitrogens trans to the two phenyl ligands. Perhaps surprisingly the Pt−C distances to the sp^2 phenyl

Table 1. Selected Bond Distances (Å) and Angles (deg) for Complex **3**

Pt1−C11	2.043 (4)	Pt1−N41	2.149 (3)
Pt1−C21	2.030 (4)	Pt1−N51	2.182 (4)
Pt1−N31	2.145 (3)		
C11−Pt1−C21	95.0 (2)	C21−Pt1−N41	175.8 (2)
C11−Pt1−N31	174.5 (2)	C21−Pt1−N51	92.5 (2)
C11−Pt1−N41	89.2 (2)	N31−Pt1−N41	85.9 (2)
C11−Pt1−N51	95.2 (2)	N31−Pt1−N51	87.0 (2)
C21−Pt1−N31	89.9 (2)	N41−Pt1−N51	86.9 (2)

Scheme 5

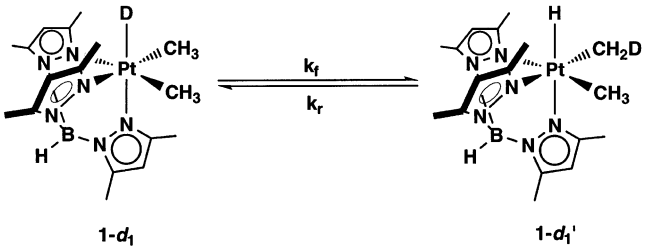

carbons of 2.043(4) and 2.030(4) Å are quite close to the sp^3 value found for the dimethyl analogue (2.048(5) Å).[23] Steric factors are surely important in the orientation of the phenyl rings and probably impact the metal−carbon distances as well.

H/D Scrambling in $Tp^{Me_2}Pt^{IV}(CH_3)_2D$ (1-d_1). The introduction of excess deuterium into the methane released in the thermolysis of **2** in C_6D_6 is consistent with a process that exchanges hydrogen atoms between hydride and methyl ligand positions prior to reductive elimination. Analogous scrambling reactions between hydride and alkyl groups have been well documented for other metal alkyl hydride complexes[12b,c,e,13,26] and recently observed for the closely related complex $TpPt^{IV}(CH_3)(H)_2$ (Tp = hydridotrispyrazolylborate) upon dissolution in CD_3OD.[27] The existence of such a process for complex **1** was directly demonstrated by equilibration of the deuteride analogue of **1**, $Tp^{Me_2}Pt^{IV}(CH_3)_2D$ (**1-d_1**), with its isotopomer, **1-d_1'** (Scheme 5).

The approach to equilibrium was monitored by ^1H NMR spectroscopy in C_6D_6 and found to be first-order ($k_{obs} = k_f + k_r = 4.1 \times 10^{-4}$ s^{-1} at 66 °C, Figure 5).[28] At 66 °C $K_{eq} = 9.9$, whereas statistics predict $K_{eq} = 6$. Thus, $Tp^{Me_2}Pt^{IV}(CH_3)(CH_2D)(H)$ (**1-d_1'**) is favored over $Tp^{Me_2}Pt^{IV}(CH_3)_2D$ (**1-d_1**) by a statistically corrected equilibrium isotope effect of 1.6 at 66 °C. This was expected, as the heavier deuterium should prefer the stronger C−D bond over the weaker Pt−D bond. Rate and equilibrium constants for the H/D scrambling reactions are listed in Table 2.[29] An Eyring plot of the temperature dependence of $k_f = (K_{eq}/(K_{eq} + 1))k_{obs}$, Figure S1, yielded activation parameters for the scrambling process of $\Delta H^{\ddagger}_{scr} = 26 \pm 1$ kcal/mol and $\Delta S^{\ddagger}_{scr} = 1 \pm 4$ cal/mol K.

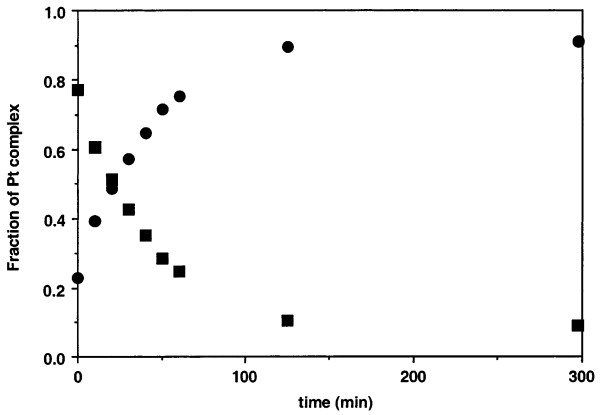

Figure 5. Disappearance of $Tp^{Me_2}Pt(CH_3)_2D$ (**1-d_1**, ■) and appearance of the isotopomer $Tp^{Me_2}Pt(CH_3)(CH_2D)H$ (**1-d_1'**, ●) in C_6D_6 at 66 °C.

Table 2. Observed Rate and Equilibrium Constants for the Thermolysis of **1-d_1**

solvent	T (°C)	k_{obs} (10^5 s^{-1})	K_{eq}	k_f (10^5 s^{-1})
C_6D_6	46.0	3.33	14	3.1
	53.0	9.41	14	8.8
	60.0	19.7	9.1	18
	66.0	40.8	9.9	37
CD_3CN/C_6F_6 (4.9 M)	60.0	6.78		

The rate of the H/D scrambling reaction depicted in Scheme 5 is not significantly affected by solvent (Table 2). The rate constant, k_{obs}, for the H/D exchange in CD_3CN/C_6F_6 (4.9 M CD_3CN) at 60.0 °C is 6.8×10^{-5} s^{-1}, approximately 3-fold slower than in C_6D_6. Qualitatively similar observations concerning H/D scrambling were made in C_6D_{12}.

Thermolysis of $Tp^{Me_2}Pt^{IV}(CH_3)_2H$ (1) in Toluene-d_8. The thermolysis reaction of **1** in toluene-d_8 was carried out at temperatures between 104.3 and 135.3 °C, and rate constants for methane reductive elimination from **1** were determined as a function of temperature. The reductive elimination process was directly monitored by following the disappearance of the hydride signal of **1** in high-temperature NMR experiments. Nearly identical activation parameters were found with respect to activation parameters measured in C_6D_6, Figure 3: $\Delta H^{\ddagger}_{obs} = 35.4 \pm 1.1$ kcal/mol and $\Delta S^{\ddagger}_{obs} = 14 \pm 3$ eu for the first methane reductive elimination. As expected, thermolysis of **1** in toluene ultimately leads to the formation of regioisomers of $Tp^{Me_2}Pt(tol)_2H$, as illustrated by signals in the high-field region of the ^1H NMR spectrum. The hydride chemical shifts for the three major isomers at −18.56 ppm ($^1J_{Pt-H} = 1365$ Hz) and −18.59 ppm (two hydride signals nearly degenerate, $^1J_{Pt-H} = 1367$ Hz) are similar to the hydride shift of $Tp^{Me_2}Pt(Ph)_2H$ (**3**)[23] and other Pt(IV) aryl dihydride species,[31] where arene activation occurs *para* or *meta* to a methyl substituent. It is reasonable to

(26) (a) Buchanan, J. M.; Stryker, J. M.; Bergman, R. G. *J. Am. Chem. Soc.* **1986**, *108*, 1537. (b) Periana, R. A.; Bergman, R. G. *J. Am. Chem. Soc.* **1986**, *108*, 7332. (c) Bullock, R. M.; Headford, C. E. L.; Hennessy, K. M.; Kegley, S. E.; Norton, J. R. *J. Am. Chem. Soc.* **1989**, *111*, 3897. (d) Parkin, G.; Bercaw, J. E. *Organometallics* **1989**, *8*, 1172. (e) Gould, G. L.; Heinekey, D. M. *J. Am. Chem. Soc.* **1989**, *111*, 5502. (f) Wang, C.; Ziller, J. W.; Flood, T. C. *J. Am. Chem. Soc.* **1995**, *117*, 1647. (g) Mobley, T. A.; Schade, C.; Bergman, R. G. *J. Am. Chem. Soc.* **1995**, *117*, 7822. (h) Chernaga, A.; Cook, J.; Green, M. L. H.; Labella, L.; Simpson, S. J.; Souter, J.; Stephens, A. H. H. *J. Chem. Soc., Dalton Trans.* **1997**, 3225. (i) Gross, C. L.; Girolami, G. S. *J. Am. Chem. Soc.* **1998**, *120*, 6605. (j) Wick, D. D.; Reynolds, K. A.; Jones, W. D. *J. Am. Chem. Soc.* **1999**, *121*, 3974. (k) Northcutt, T. O.; Wick, D. D.; Vetter, A. J.; Jones, W. D. *J. Am. Chem. Soc.* **2001**, *123*, 7257. (l) Jones, W. D. *Acc. Chem. Res.* **2003**, *36*, 140. (m) Churchill, D. G.; Janak, K. E.; Wittenberg, J. S.; Parkin, G. *J. Am. Chem. Soc.* **2003**, *125*, 1403.

(27) (a) Lo, H. C.; Haskel, A.; Kapon, M.; Keinan, E. *J. Am. Chem. Soc.* **2002**, *124*, 3226. (b) Iron, M. A.; Lo, H. C.; Martin, J. M. L.; Keinan, E. *J. Am. Chem. Soc.* **2002**, *124*, 7041

(28) Approximately 20% of the material had already scrambled to **1-d_1'** by the start of the data collection shown in Figure 5. This scrambling occurs during sample preparation and the time required for temperature stabilization in the heated NMR probe.

(29) The irregular variation in the K_{eq} values with temperature results from the fact that the experimental numbers are large (i.e., reaction proceeds almost to completion). This uncertainty does not have a significant effect on k_f as $k_f = (K_{eq}/(K_{eq} + 1))k_{obs}$ where $K_{eq}/(K_{eq} + 1)$ is near unity.

Scheme 6

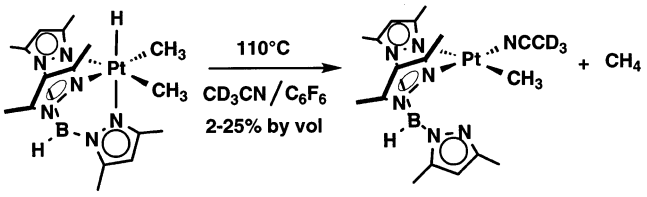

assign these three signals to $Tp^{Me_2}Pt(tol)_2H$ isomers, in which toluene is activated preferentially in the *meta* and *para* positions for steric reasons, thus giving rise to p-tol/p-tol, m-tol/p-tol, and m-tol/m-tol isomers. We have observed that in cases where single *ortho* isomer arene C−H activation products can be isolated, the hydride chemical shift of $Tp^{Me_2}Pt(aryl)(H)_2$ moves significantly upfield to about −19.2 ppm when a substituted arene such as *p*-xylene is C−H activated *ortho* to the methyl substituent. The NMR chemical shift for the two minor hydride resonances in $Tp^{Me_2}Pt(tol)_2H$ at −19.35 and −19.39 ppm ($^1J_{Pt-H}$ = 1366 Hz) could thus be attributed to the two o-tol/p-tol and o-tol/m-tol isomers, if one discards the formation of the o-tol/o-tol isomer for steric reasons. No attempts to separate the complex $Tp^{Me_2}Pt(tol)_2H$ isomer mixture were made.

Thermolysis of $Tp^{Me_2}Pt^{IV}(CH_3)_2H$ (1) in Acetonitrile/Hexafluorobenzene Mixtures. Thermolysis of $Tp^{Me_2}Pt^{IV}(CH_3)_2H$ (**1**) in neat CD_3CN was complicated by side reactions and variable incorporation of deuterium atoms from the solvent into the platinum-hydride position. However, when diluted with C_6F_6 such that the concentration of CD_3CN was less than 5 M (ca. 26 vol %), the reaction proceeded cleanly to produce κ^2-$Tp^{Me_2}Pt^{II}(CH_3)(NCCD_3)$[30] (**4**) and CH_4 (Scheme 6). Spectroscopic yields of the Pt(II) acetonitrile adduct **4** were quantitative under these conditions.

The loss of mirror-plane (C_s) molecular symmetry in the conversion of **1** to **4** was clearly indicated as the 2:1 Tp^{Me_2} spectral symmetry changed to 1:1:1. Dissociation of one pyrazolyl nitrogen from Pt(II) in **4** results in pronounced upfield shifts of the three resonances arising from the detached ring and disappearance of ^{195}Pt coupling to the methine signal. The coordinated solvent ligand was observed by carrying out the reaction with CH_3CN and examining the nonvolatile products in C_6D_6. The ^{1}H NMR data matched those previously reported for **4**.[30]

The thermal reaction of **1** in mixtures of CD_3CN/C_6F_6 followed first-order kinetic behavior with respect to the disappearance of **1**. The rate constant of this first-order reaction to yield methane and **4** at 110.0 °C was measured with CD_3CN concentrations ranging from 0.56 to 4.9 M. There was no observed dependence of the rate on the CD_3CN concentration and $k_{obs} = 5.10 \pm 0.04 \times 10^{-5}$ s^{-1} for these experiments (Table S1, Figure S2).

Thermolysis of $Tp^{Me_2}Pt^{IV}(CH_3)_2H$ (1) in Cyclohexane-d_{12}. Thermolysis of $Tp^{Me_2}Pt(CH_3)_2H$ (**1**) in cyclohexane-d_{12} at 100 °C resulted in a first-order decomposition reaction that released methane with an observed rate ($k_{obs} = 5.14 \times 10^{-5}$ s^{-1}) comparable to that obtained in benzene-d_6. Aliphatic C−D bond activation was demonstrated by the observation of ^{1}H NMR signals of the deuterated methanes, CH_3D, CH_2D_2, and CHD_3. However, resonances assignable to the expected organoplatinum(IV) alkyl deuteride species $Tp^{Me_2}Pt(CH_3)(C_6D_{11})D$, $Tp^{Me_2}Pt(D)(C_6D_{11})_2$, or their isotopomers were not observed. Instead, significant quantities of black platinum metal eventually precipitated from solution. ^{1}H NMR signals arising from at least two new platinum complexes were detected during the course of the reaction. Initial accumulation of a broad Pt−H resonance at −19.50 ppm (J_{Pt-H} = 1309 Hz) appeared to coincide with the appearance of a Pt−CH_3 signal at 1.70 ppm (J_{Pt-H} = 70.6 Hz) and a set of Tp^{Me_2} ligand signals with 2:1 symmetry. Somewhat later, a signal appeared at −20.09 ppm (J_{Pt-H} = 1176 Hz), possibly due to a Pt(II)−H species.[33] These intermediates displayed complex kinetic behavior that was variable between experiments, and other minor unassigned resonances were also observed. Thermolysis of **1** in cyclohexane (C_6H_{12}) for 5 days at 115 °C followed by distillation of the volatile products away from the black residue produced cyclohexene as the major organic product detectable in the ^{1}H NMR spectrum.

The chemistry was greatly simplified by the addition of an excess of PPh_3 to a cyclohexane-d_{12} solution of **1**. Significantly, the rate of the disappearance of **1** was not affected by the presence of 0.3 M $P(C_6D_5)_3$ (Table S1). However, no platinum black was formed and no $Tp^{Me_2}Pt$ intermediates were observed; the solution instead turned yellow and a yellow solid precipitated as the reaction progressed. The products observed by ^{1}H NMR spectroscopy were methane, deuterated methane isotopomers, and HTp^{Me_2}, the latter indicated by singlets at 2.08, 5.54, and 12.58 ppm, assignable to the methyl, methine, and pyrazoylium protons, respectively. A ^{31}P NMR spectrum of the product mixture indicated the presence of multiple soluble Pt phosphine complexes that have not been further characterized.

Thus, the thermolysis of **1** in cyclohexane-d_{12} results in the reductive elimination of methane both in the presence and absence of phosphine. The similar rates with and without added PPh_3, together with the observation of the deuterated methane isotopomers in both cases, point to a Pt(II) intermediate being involved in C−D bond activation of the aliphatic solvent.

Discussion

Oxidative addition of a C−H bond to a Pt(II) center to form a Pt(IV) alkyl hydride species has been proposed as the initial activation step in platinum-catalyzed alkane oxidation reactions.[2,6] While there have been several reports of hydrocarbon activation by Pt(II) centers,[8−10] reports of oxidative addition of hydrocarbon C−H bonds to Pt(II) to form stable Pt(IV) alkyl hydride and aryl hydride species are rare.[21,24e,f,31] This paucity of model systems has inhibited detailed study of the reaction. However, significant details about the intimate mechanism of this reaction can be obtained through the study of the microscopic reverse process, C−H reductive elimination of alkanes from Pt(IV) alkyl hydrides. Recently, a number of elegant studies have approached the investigation of C−H reductive elimination via protonation of Pt(II) alkyl complexes.[6,11−13] Unfortunately, these studies are often complicated by the instability of the Pt(IV) alkyl hydride complexes generated in situ; in some cases, direct detection of the Pt(IV) species generated by protonation was not possible.[11] In addition, since

(30) Reinartz, S.; White, P. S.; Brookhart, M.; Templeton, J. L. *Organometallics* **2000**, *19*, 3854.

(31) Reinartz, S.; White, P. S.; Brookhart, M.; Templeton, J. L. *Organometallics* **2001**, *20*, 1709.

Scheme 7

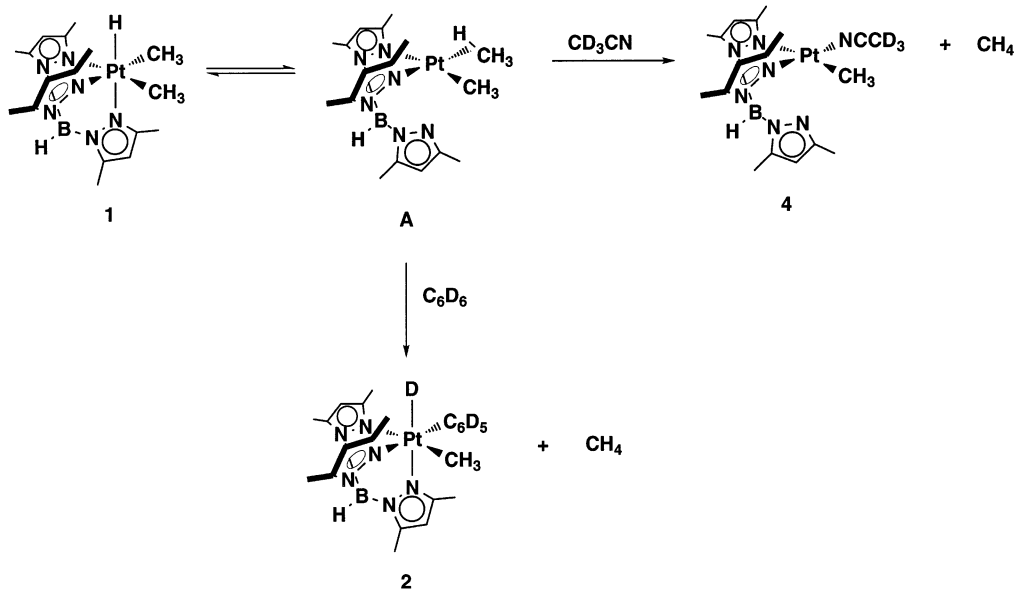

the protonated species from which C−H reductive elimination was observed are cationic, the study of these C−H bond forming reactions in hydrocarbon solvents has been difficult.

In contrast, the neutral alkyl hydride $Tp^{Me_2}Pt^{IV}(CH_3)_2H$ (**1**) is remarkably stable and is soluble in nonpolar solvents.[23] Reductive eliminations of alkanes from Pt(IV) often proceed via five-coordinate intermediates formed by preliminary ligand dissociation.[12−17,32] The high barrier to dissociation of a pyrazolyl arm to form a five-coordinate Pt(IV) intermediate is likely a key factor in the enhanced stability of **1**. This rationale is also consistent with the report that protonation of **1** prompts rapid reductive elimination of methane at −78 °C; protonation at one pyrazolyl arm of the Tp^{Me_2} ligand generates a reactive five-coordinate species that rapidly undergoes C−H coupling.[30] The Pt(II) product of this reaction can be trapped by exogenous ligands to generate stable $[\kappa^2\text{-}(HTp^{Me_2})Pt^{II}(CH_3)L]BAr'_4$ complexes,[30] and similar reactions with $Tp^{Me_2}Pt^{IV}Me(H)_2$ have been reported.[33]

In the absence of added acid, temperatures in excess of 100 °C are required to promote reductive elimination of methane from **1**. The rate of this thermal C−H reductive elimination reaction is relatively insensitive to solvent (Table S1), even though the platinum product is determined by the solvent (Scheme 7). The Pt(II) product of reductive elimination is trapped by acetonitrile to form the solvent adduct $\kappa^2\text{-}Tp^{Me_2}Pt^{II}(CH_3)(NCCD_3)$ (**4**). In contrast, oxidative addition of a C−D bond occurs in hydrocarbon solvents such that with C_6D_6 the Pt(IV) aryl deuteride $\kappa^3\text{-}Tp^{Me_2}Pt^{IV}(CH_3)(C_5D_5)(D)$ (**2-*d*$_6$**) forms (Scheme 7). Alkane C−D bond activation was observed when cyclohexane-d_{12} was employed as the solvent, but the expected Pt(IV) hydrocarbyl product was unstable under the reaction conditions, and a significant amount of Pt(0) was produced.

Scrambling of hydrogen atoms between the methyl and the hydride positions of **1** occurs at lower temperatures (ca. 60 °C). This scrambling reaction and the reductive elimination are proposed to proceed via a common intermediate, the σ-methane complex $\kappa^2\text{-}Tp^{Me_2}Pt^{II}(CH_3)(CH_4)$. A similar intermediate, $\kappa^2\text{-}TpPt^{II}(D)(CH_3D)$, was proposed in H/D scrambling reactions of the closely related complex $\kappa^3\text{-}TpPt^{II}(H)_2(CH_3)$ in CD_3OD.[27] The presence of this σ-complex intermediate on the reaction pathway and the mechanism of the release of methane have important implications for the microscopic reverse reaction, the oxidative addition of C−H bonds to Pt(II) complexes.

Scheme 8

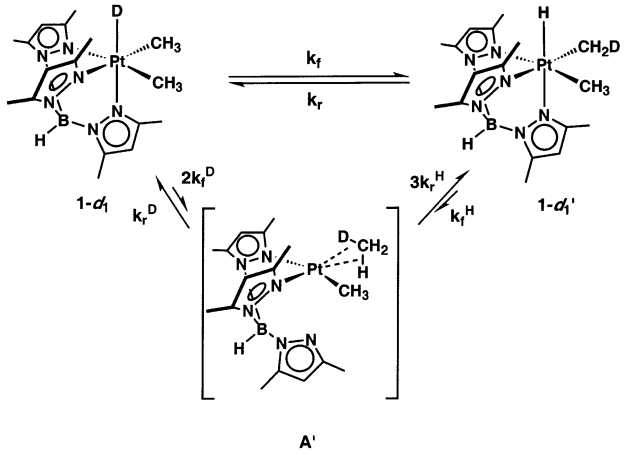

Hydrogen Scrambling between the Hydride and the Methyl Positions of 1. When the complex $\kappa^3\text{-}Tp^{Me_2}Pt^{IV}(CH_3)_2D$ (**1-*d*$_1$**) was heated in solution (45−65 °C), H/D scrambling occurred to form an equilibrium mixture of starting material and $\kappa^3\text{-}Tp^{Me_2}Pt(CH_3)(CH_2D)H$ (**1-*d*$_1$′**). The four-coordinate methane complex $\kappa^2\text{-}Tp^{Me_2}Pt^{II}(CH_3)(CH_3D)$ (**A′**, Scheme 8) is proposed as an intermediate in this reaction. Alkane σ-complexintermediates have been invoked to explain H/D scrambling reactions observed for a variety of isotopically labeled late metal alkyl hydride complexes.[12b,c,e,13,26,27] Inverse kinetic isotope effects for the C−H(D) reductive elimination reactions have been reported in cases in which prior H/D scrambling occurs.[13,26] Such inverse isotope effects are compatible with the presence of a σ-alkane intermediate on the reaction pathway to reductive elimination.[26,34] Our observations of deuterium scrambling

(32) Fekl, U.; Goldberg, K. I. *J. Am. Chem. Soc.* **2002**, *124*, 6804.
(33) Reinartz, S.; Baik, M.-H.; White, P. S.; Brookhart, M.; Templeton, J. L. *Inorg. Chem.* **2001**, *40*, 4726.

between the hydride and methyl positions and an inverse kinetic isotope effect for reductive elimination of methane from **1** can be accommodated by invoking a common alkane σ-complex intermediate in these reactions.

The structure of the intermediate **A′** pictured in Scheme 8 is drawn with an η^2-H,D methane. An alternative structure would be an η^2-C,D(H) methane complex (**A** in Scheme 7). Either structure could be the ground state of the intermediate, as calculations on such σ-complexes indicate that they lie in a shallow energy surface and rapid conversion between these different structures is expected.[35,36] The κ^2-Tp^{Me_2} configuration shown for intermediate **A** (or **A′**) is consistent with the square-planar coordination geometry generally preferred for a Pt(II) center. A number of neutral Pt(II) complexes with an ancillary tris(pyrazolyl)borate ligand have been isolated, and available crystal structures of such species illustrate this bidentate coordination mode of the Tp ligand.[30,37]

The structure of the σ-methane complex is reminiscent of a closely related Pt(II) benzene adduct, $[\kappa^2$-$(HTp^{Me_2})Pt^{II}H(\eta^2$-$C_6H_6)]^+$, which has been crystallographically characterized.[38a] In this cationic complex, one pyrazolyl ring is protonated and a pseudo-square-planar environment around the platinum is obtained. The hydrocarbon C−C bond occupies one of the four sites in the square plane. Hydrogen exchange reactivity, analogous to that observed for **1**, is also found for $[\kappa^2$-(HTp^{Me_2})-$Pt^{II}H(\eta^2$-$C_6H_6)]^+$. The Pt(II) cation undergoes exchange of the hydrogen in the hydride position with the hydrogens on the coordinated benzene. This process was proposed to proceed via oxidative addition to form a five-coordinate dihydrido phenyl Pt(IV) intermediate.[38] Note that the proton on the pyrazolyl of $[\kappa^2$-$(HTp^{Me_2})Pt^{II}H(\eta^2$-$C_6H_6)]^+$ prevents the five-coordinate Pt-(IV) phenyl hydride intermediate from achieving stabilization as a six-coordinate κ^3-Tp^{Me_2} species. As a result the κ^2-ligated Pt(II) hydrocarbon adduct is the ground state and the Pt(IV) phenyl hydride is the proposed intermediate. The situation is reversed in the present work, where the κ^3-Tp^{Me_2}Pt(IV) species

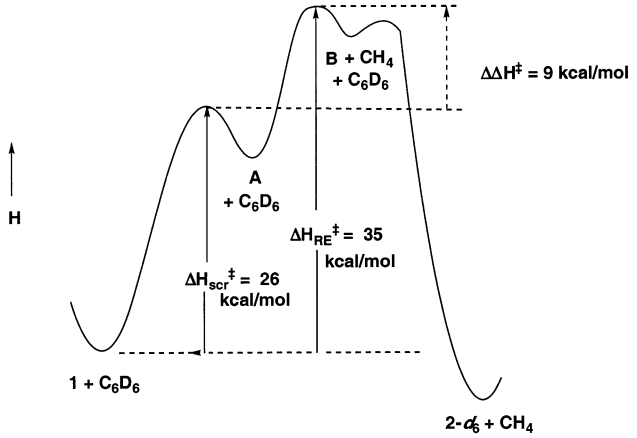

Figure 6. Enthalpy diagram for the conversion of **1** to **2-d_6** in C_6D_6 solvent.

1 is the ground state and the κ^2-ligated Tp^{Me_2} Pt(II) hydrocarbon adduct is an intermediate.

Scrambling of deuterium between the hydride position and the methyl groups of complex **1-d_1** was observed to be a first-order process. The reaction proceeds nearly to completion (average $K_{eq} = 12 \pm 3$), so that k_f comprises approximately 90% of the magnitude of k_{obs}. Activation parameters of $\Delta H^{\ddagger}_{scr} = 26 \pm 1$ kcal/mol and $\Delta S^{\ddagger}_{scr} = 1 \pm 4$ eu were calculated from an Eyring plot of these k_f values (Figure 6). The forward rate constant, k_f, is limited by formation of the σ-methane complex, k_f^D, from **1-d_1** (Scheme 8). This is consistent with the fact that the σ-methane complex intermediate is not observed and also with calculations and experimental results that find a small activation energy for oxidative addition of coordinated C−H bonds.[35,36] Thus, the activation parameters calculated from the k_f values can be considered a reasonable estimate of the barrier to the alkane complex formation. This barrier does not correspond to a simple C−H reductive coupling reaction, as pyrazolyl dissociation would represent a substantial portion of the enthalpic barrier to formation of the σ-methane intermediate **A**.

Elimination of the Bound Methane from the Pt(II) Alkane σ-Complex Intermediate. The remarkably large difference of ca. 40 °C in the temperatures required for the isotope exchange and methane elimination reactions allows for an unusually detailed study of the alkane release step. In particular, it allows us to address the question of whether the methane loss occurs via a dissociative pathway from the σ-methane complex **A** or via a nucleophilic displacement by an incoming solvent molecule.

As detailed in Scheme 9, an incoming ligand (e.g., acetonitrile) can either displace methane from the σ-complex intermediate (k_2) or enter the open coordination site left by departure of methane (k_3). In principle, these mechanisms can be distinguished by the dependence of the observed rate on acetonitrile concentration. For a reaction that proceeds via the dissociative path, the rate should be independent of acetonitrile concentration, as acetonitrile binds only after rate-determining methane loss ($k_{obs} = (k_1/k_{-1})k_3$). This is consistent with our experimental observations; rates of the thermolysis of **1** in mixtures of CH_3CN/C_6F_6 to form the Pt(II) complex κ^2-$Tp^{Me_2}Pt^{II}(CH_3)(NCCD_3)$ (**4**) were constant over an order of magnitude variation in acetonitrile concentration (0.56−4.9 M). However, an associative pathway could also exhibit a rate independent of acetonitrile

(34) While it is possible to obtain an inverse kinetic isotope effect in a single reaction step, a more reasonable explanation is a two-step mechanism whereby the observed isotope effect is then a product of the equilibrium isotope effect between the starting and intermediate complexes and the kinetic isotope effect of a rate-determining second step.[26] In this way, an inverse equilibrium isotope effect can dominate in the kinetic isotope effect measured for the overall reductive elimination reaction. An alkane σ-complex is an ideal intermediate in this context; the significantly greater strength of the methane carbon−hydrogen bond in the σ-alkane complex, relative to the metal−hydrogen bond in the starting complex, leads to the requisite inverse equilibrium isotope effect. Note that *kinetic* isotope effects of the forward and reverse reactions of this preequilibrium between the alkyl hydride complex and the σ-alkane complex can both be normal.[26k,l] Loss of the alkane from the σ-complex in the second and rate-determining step of reductive elimination should not have a significant effect on the C−H bond, so only a small, primary kinetic isotope effect is expected.

(35) See references cited in: (a) Kubas, G. J. *Metal Dihydrogen and σ-bond Complexes*; Kluwer Academic/Plenum: New York, 2001; Chapters 7 and 12. (b) Hall, C.; Perutz, R. N. *Chem. Rev.* **1996**, *96*, 3125.

(36) For some examples with Pt(II)/Pt(IV) see: (a) Siegbahn, P. E. M.; Crabtree, R. H. *J. Am. Chem. Soc.* **1996**, *118*, 4442. (b) Hill, G. S.; Puddephatt, R. J. *Organometallics* **1998**, *17*, 1478. (c) Heiberg, H.; Swang, O.; Ryan, O. B.; Gropen, O. *J. Phys. Chem. A* **1999**, *103*, 10004. (d) Bartlett, K. L.; Goldberg, K. I.; Borden, W. T. *J. Am. Chem. Soc.* **2000**, *122*, 1456. (e) Mylvaganam, K.; Bacskay, G. B.; Hush, N. S. *J. Am. Chem. Soc*. **2000**, *122*, 2041. (f) Heiberg, H.; Johansson, L.; Gropen, O.; Ryan, O. B.; Swang, O.; Tilset, M. *J. Am. Chem. Soc*. **2000**, *122*, 10831. (g) Gilbert, T. M.; Hristov, I.; Ziegler, T. *Organometallics* **2001**, *20*, 1183. (h) Bartlett, K. L.; Goldberg, K. I.; Borden, W. T. *Organometallics* **2001**, *20*, 2669. (i) Kua, J.; Xu, X.; Periana, R. A.; Goddard, W. A., III. *Organometallics* **2002**, *21*, 511. (j) Ref 27b.

(37) Oliver, J. D.; Rush, P. E. *J. Organomet. Chem*. **1976**, *104*, 117.

(38) (a) Reinartz, S.; White, P. S.; Brookhart, M.; Templeton, J. L. *J. Am. Chem. Soc*. **2001**, *123*, 12724. (b) Norris, C. M.; Reinartz, S.; White, P. S.; Templeton, J. L. *Organometallics* **2002**, *21*, 5649.

Scheme 9

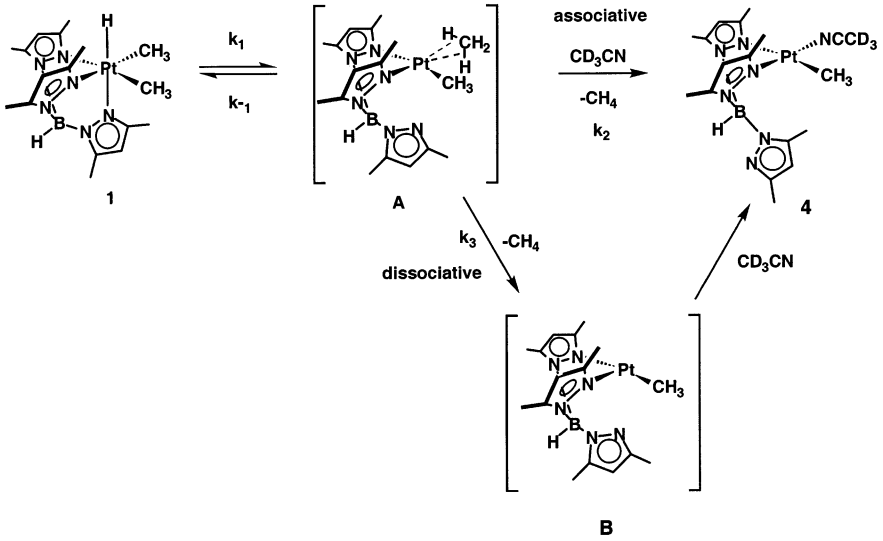

concentration if the first step of the reaction, formation of the σ-methane complex, is rate-limiting (i.e., conditions of saturation kinetics, $k_{obs} = k_1$). In this case, the rate of the overall reductive elimination reaction ($k_{obs} = 5.1 \times 10^{-5}$ s^{-1} at 110 °C) would be limited by the rate of the formation of the σ-methane complex. However, the measured rate constant for the H/D scrambling reaction attains this value at a temperature 50 deg lower in the same solvent system ($k_{obs} = 7 \times 10^{-5}$ s^{-1} at 60 °C). Thus, k_1 must greatly exceed k_{obs} for C−H reductive elimination of methane at 110 °C, and an associative mechanism for methane loss is not consistent with these data.

Other observations are also more consistent with a dissociative mechanism. Observed rates of methane loss from **1** in solvents of different donor abilities (benzene, toluene, cyclohexane, acetonitrile/hexafluorobenzene) varied only slightly at 110 °C (Table S1, Figure 3). The rate of reaction was unaffected by the addition of 0.3 M PPh_3, in cyclohexane-d_{12}. Finally, there is no significant substituent effect ($-CH_3$ vs $-C_6D_5$) on the consecutive methane displacements in benzene-d_6; the observed activation parameters are almost identical. In the thermolysis of **1-*d*$_7$** at 110 °C, where there is no contribution from a variable isotope effect, the elimination from the more bulky phenyl derivative **2-*d*$_9$** is actually slightly faster than from **1-*d*$_7$** (ca. 30%). Thus, all of our evidence is consistent with a dissociative mechanism for rate-determining methane loss from the σ-complex intermediate.

In contrast to the results of our study, the vast majority of substitution reactions at Pt(II) proceed via an associative mechanism.[39] In fact, support was recently presented for associative displacement of methane from a cationic diimine Pt(II) σ-complex intermediate.[11a] A negative activation volume, indicative of an associative mechanism, was also recently reported for substitution of a weakly bound solvent molecule by benzene at a cationic Pt(II) center.[11b] However, there are several well-characterized examples of dissociative substitution and isomerization pathways for square-planar Pt(II) complexes.[40] These reactions typically have strong donors (alkyls or aryls) trans to the leaving group. While this is not the case for κ^2-$Tp^{Me_2}Pt(CH_3)(CH_4)$, methane constitutes such an excellent leaving group that a strong trans director may not be necessary to promote the dissociative reaction. Furthermore, the cationic diimine species previously shown to undergo associative alkane displacement[11] should exhibit greater electrophilicity than the neutral Tp^{Me_2} Pt(II). Notably, an analogous arene displacement from a neutral Ir(I) complex has also been shown to proceed via a dissociative mechanism.[41] Ligand steric factors may be an additional contributing factor. The free pyrazolyl arm or possibly the bulk of the coordinated dimethylpyrazolyl rings may block the approach of a nucleophile to κ^2-$Tp^{Me_2}Pt(CH_3)(CH_4)$ and so contribute to a higher barrier to an associative substitution pathway. Thus, although associative substitution is more common at d^8 square-planar centers, certain combinations of metal, charge, and ligand set can favor a dissociative mechanism.

Finally, the possibility that the free pyrazolyl arm actually contributes to promoting dissociative methane loss via anchimeric assistance must be considered. In fact, recent DFT calculations on the hypothetical methane elimination from κ^3-$TpPt^{IV}(CH_3)(H)_2$ provide support for the active participation of the dissociated pyrazolyl arm.[27b] The free energies of the three-coordinate (T-shaped) κ^2-$TpPt^{II}(H)$ and four-coordinate (seesaw shaped) κ^3-$TpPt^{II}(H)$ were found to be nearly identical ($\Delta\Delta G_{298} = 0.6$ kcal/mol favoring the κ^2 form). Moreover, the calculations found that the Tp ligand in the transition state for methane loss from κ^2-$TpPt(H)(CH_4)$ is coordinated in a κ^3 fashion. This suggests that methane loss proceeds directly from the σ-alkane complex to the κ^3-$TpPt^{II}(H)$ structure. This trajectory can be viewed as an intramolecular associative interchange type displacement of methane that is distinctive from a true substitution since the product cannot assume a stable square-planar geometry. Relaxation of this species to the κ^2-$TpPt^{II}(H)$ structure after departure of methane eventually accommodates coordination of an exogenous ligand to yield the κ^2-$TpPt^{II}(H)(L)$ product. It is also of significant interest that the calculations yielded activation energies for methane complex formation, κ^2-$TpPt^{II}(CH_4)(H)$ from κ^3-$TpPt^{II}(CH_3)(H)_2$ ($\Delta G^{\ddagger}_{298} = 25.7$ kcal/mol),

(39) Atwood, J. D. *Inorganic and Organometallic Reaction Mechanisms*, 2nd ed.; Wiley: New York, 1997; Chapter 2.
(40) See for example: (a) Romeo, R. *Comments Inorg. Chem.* **1990**, *11*, 21. (b) Alibrandi, G.; Scolaro, L. M.; Romeo, R. *Inorg. Chem.* **1991**, *30*, 4007.
(41) Kanzelberger, M.; Singh, B.; Czerw, M.; Krogh-Jespersen, K.; Goldman, A. S. *J. Am. Chem. Soc.* **2000**, *122*, 11017.

as well as for the elimination of methane ($\Delta G^{\ddagger}_{298} = 31.0$ kcal/mol), that are virtually identical to the experimental kinetic barriers measured in this work for very similar complexes (vide infra). Thus, anchimeric assistance by the Tp ligand may provide the best explanation for the unusual dissociative substitution of methane described here.[42]

Dissociation of methane from κ^2-$Tp^{Me_2}Pt^{II}(CH_3)(CH_4)$ would yield the three-coordinate [κ^2-$Tp^{Me_2}Pt(CH_3)$] fragment (**B** in Scheme 9) or possibly the four-coordinate [κ^3-$Tp^{Me_2}Pt(CH_3)$].[43] This $Tp^{Me_2}Pt(CH_3)$ species is presumably similar to the reactive species in the organoborane-mediated hydrocarbon activation observed upon reaction of K[κ^2-$Tp^{Me_2}Pt(CH_3)_2$] with $B(C_6F_5)_3$ in hydrocarbon solvent.[21] The difference in enthalpies between this unsaturated metal species and the methane σ-complex corresponds to the binding enthalpy of methane to the Pt(II) center. A lower limit for this binding enthalpy is obtained from the difference in the activation enthalpies for H/D scrambling between the hydride and methyl positions and the reductive elimination of methane, $\Delta\Delta H^{\ddagger} = \Delta H^{\ddagger}_{RE} - \Delta H^{\ddagger}_{scr} = 9 \pm 2$ kcal/mol. This is depicted in the energy diagram for the reaction of **1** in C_6D_6 to form **2** (Figure 6). This value serves as a lower limit because there is no information available as to the depth of the energy well corresponding to the σ-alkane complex (**A**). However, theoretical calculations suggest a minimal barrier to oxidative addition of methane coordinated to Pt(II),[36] and this is experimentally supported by the observation of reversible oxidative addition of benzene in [κ^2-$(HTp^{Me_2})Pt^{II}H(\eta^2$-$C_6H_6)$]$^+$ at low temperature.[38] Thus, this estimate of the minimum methane binding enthalpy is likely close to the true value. This is the first experimental estimate of an alkane binding enthalpy to Pt(II). It is in good agreement with previous theoretical estimates of methane binding to Pt(II) and other experimental measurements and estimates of methane binding enthalpies to transition metal centers.[35,36]

Trapping of the Pt(II) Product. The reaction sequence can be completed by addition of a two-electron donor ligand to the three-coordinate Pt(II) intermediate to form a square-planar Pt(II) complex. With acetonitrile, a solvento adduct, κ^2-$Tp^{Me_2}Pt(CH_3)(NCCD_3)$ (**4**), was produced. In contrast, a hydrocarbon solvent yields products of C−H bond activation. By analogy with the displaced methane, an electron pair in a C−H bond of the solvent can act as a trapping ligand. Subsequent oxidative addition occurs to generate a Pt(IV) product. This was observed in benzene solvent, and κ^3-$Tp^{Me_2}Pt^{IV}(CH_3)(C_6D_5)(D)$ (**2-*d*$_6$**) was obtained. Reductive elimination of a second equivalent of methane from this intermediate Pt(IV) species can occur. Formation of isotopomers of **2-*d*$_6$** involving the hydride and phenyl ring positions and the observation of the subsequent reductive elimination of CD_2H_2 in addition to CH_3D suggest that the oxidative addition of benzene is reversible and the intermediate κ^2-$Tp^{Me_2}Pt(CH_2D)(C_6D_5H)$ is involved. In contrast to the behavior of the proposed σ-methane complex, exchange of bound benzene with solvent was not observed on the thermolysis time scale, as no accumulation of free C_6D_5H was noted. This implies that the binding of benzene to the intermediate κ^2-$Tp^{Me_2}Pt(CH_3)$ is significantly stronger than that of methane, a conclusion that is consistent with qualitative expectations and further supported by the recent isolation of [κ^2-$(HTp^{Me_2})PtH(\eta^2$-$C_6H_6)$]$^+$ formed by acid-promoted reductive elimination from κ^3-$Tp^{Me_2}Pt^{IV}(C_6H_5)(H)_2$.[38] An analogous methane complex was not observed in similar acid-promoted reductive elimination from κ^3-$Tp^{Me_2}Pt^{IV}(CH_3)(H)_2$.

Thermolysis of **1** in cyclohexane-d_{12} also results in rate-limiting reductive elimination of methane (CH_4) and presumably forms the unsaturated intermediate [$Tp^{Me_2}Pt^{II}(CH_3)$]. Reaction of K[κ^2-$Tp^{Me_2}Pt^{II}(CH_3)_2$] with $B(C_6F_5)_3$ in the presence of aliphatic and aromatic C−H bonds at 25−50 °C is known to produce the oxidative addition products κ^3-$Tp^{Me_2}Pt^{IV}(CH_3)(R)(H)$ (R = phenyl, cyclohexyl, pentyl, Scheme 2).[21] Similarly, elimination of the methane isotopomers, CH_3D, CH_2D_2, and CHD_3, during thermolysis of **1** at 110 °C indicates that the product of methane loss from **1** is capable of activating aliphatic as well as aromatic C−H(D) bonds. However, the expected κ^3-$Tp^{Me_2}Pt^{IV}(CH_3)(C_6D_{11})(D)$ product is apparently unstable at elevated temperatures and decomposes rapidly, ultimately forming Pt(0) in the absence of a trapping ligand. This observation suggests that the cyclohexyl-d_{11} moiety can access a decomposition pathway that is not available to the phenyl analogue. A β-deuteride elimination reaction has considerable precedent in this regard and would account for the excess deuterium found in the methane product. Confirmation of the presence of cyclohexene, the expected product of β-hydride elimination from the Pt(II) intermediate that would form from $Tp^{Me_2}Pt^{IV}(CH_3)(C_6H_{11})H$ following methane loss, was achieved in an NMR experiment. The precipitation of platinum black from cyclohexane solution coupled with the observation of cyclohexene as the major organic product is consistent with the β-hydride decomposition hypothesis.

Summary

Thermolysis of the Pt(IV) alkyl hydride complex κ^3-$Tp^{Me_2}Pt^{IV}(CH_3)_2(H)$ (**1**) leads to reductive elimination of methane. A lower energy C−H bond forming and cleaving process scrambles hydrogen atoms between the hydride and methyl positions of **1**. A common Pt(II) σ-methane complex, κ^2-$Tp^{Me_2}Pt^{II}(CH_3)(CH_4)$ (**A**), is proposed as an intermediate in both the hydrogen scrambling and the reductive elimination reactions.

Our data are consistent with loss of methane from κ^2-$Tp^{Me_2}Pt^{II}(CH_3)(CH_4)$ (**A**) as the rate-determining step in the methane reductive elimination reaction. Methane loss from this intermediate by a dissociative pathway, possibly with anchimeric assistance from the Tp ligand, is postulated. The resulting unsaturated κ^2- or κ^3-$Tp^{Me_2}Pt^{II}(CH_3)$ fragment can be trapped by a wide range of solvent molecules. When the solvent (S) can act as an electron pair donor, the Pt(II) product κ^2-$Tp^{Me_2}Pt^{II}(CH_3)(S)$ is observed. When a hydrocarbon solvent (R−D) is employed, a C−D bond of the solvent acts as a ligand to form κ^2-$Tp^{Me_2}Pt^{II}(CH_3)(RD)$ as an intermediate, which rapidly undergoes oxidative addition of the C−D bond to generate the Pt(IV) complex κ^3-$Tp^{Me_2}Pt^{IV}(CH_3)(R)(D)$. In the case of arenes, these Pt(IV) complexes can be characterized. With cyclohexane-d_{12}, the corresponding Pt(IV) alkyl hydride complex was not observed, but the observation of CH_3D along with the other isotopomers of methane indicates that the C−D bonds of the

(42) A reviewer has suggested that the data could also be accommodated by an associative methane substitution pathway if the rate-limiting step is actually a ligand isomerization that provides steric access to the Pt center. This possibility cannot be excluded, but it should be noted that this isomerization must require more energy than dissociation of methane from the metal center.

(43) If the calculations on the κ^2 and κ^3 forms of TpPtH[27b] can be related to the current system, only a very small energy difference is expected between these two coordination environments in the $Tp^{Me_2}Pt(CH_3)$ fragment.

alkane were activated by the unsaturated [$Tp^{Me_2}Pt^{II}(CH_3)$] fragment generated upon methane loss from **1**.

Enthalpic barriers to both the scrambling and the reductive elimination processes were determined. Together these afford an estimate of methane binding enthalpy to the Pt(II) $Tp^{Me_2}Pt(CH_3)$ fragment of ca. 9 kcal/mol. Note that the scrambling barrier and the reductive elimination barrier both have a significant contribution from the binding enthalpy of the third pyrazolyl arm. Thus, as previously proposed, the unusual stability of the Pt(IV) alkyl hydride complex **1** is due in large part to the strong κ^3 chelate effect of the Tp^{Me_2} ligand.

Experimental Section

General Considerations. Unless otherwise noted, all manipulations were performed in a Vacuum-Atmospheres drybox equipped with an oxygen and water scavenging system, or on a vacuum line. ^{1}H NMR spectra were recorded on a Bruker WM-500 spectrometer operating at 500 MHz and utilizing Techmag software with the exception of the toluene kinetics NMR data, which were obtained on an Bruker Avance 400. All materials were purchased as the highest possible grade and were used as received, except for routine drying and degassing of solvents. Deuterated NMR solvents were dried by analogous methods and transferred under vacuum. [(μ-Me_2S)$Pt(CH_3)_2$]$_2$ was prepared by a literature procedure.[44]

Synthesis of $Tp^{Me_2}Pt(CH_3)_2(H)$ (1). This compound was prepared by a modification of the literature procedure.[23] Solid samples of [(μ-Me_2S)$Pt(CH_3)_2$]$_2$ (0.101 g, 0.176 mmol) and KTp^{Me_2} (0.118 g, 0.351 mmol) were placed into a 50 mL glass vessel equipped with a sidearm to a resealable Teflon valve. The vessel was evacuated, and dry acetone (5 mL) was condensed into the flask using liquid N_2. The bomb was sealed, warmed to room temperature, and gently shaken to dissolve all solids. The yellow solution was allowed to stand at room temperature, and colorless, block crystals of $Tp^{Me_2}Pt(CH_3)_2(H)$ were deposited within hours. The mother liquor was decanted, and the crystals were washed with cold acetone and dried under vacuum for 3 h. The crystals were recovered in a drybox, 0.100 g (0.191 mmol, 54%). Spectral data matched that previously reported.[23]

Preparation of $Tp^{Me_2}Pt(CH_3)_2(D)$ (1-d_1) and $Tp^{Me_2}Pt(CD_3)_2(D)$ (1-d_7). The procedure described above yields $Tp^{Me_2}Pt(CH_3)_2(D)$ (**1-d_1**) when acetone-d_6 is substituted as the solvent. $Tp^{Me_2}Pt(CD_3)_2(D)$ (**1-d_7**) was obtained by heating an acetone-d_6 solution of **1** to 65 °C for 15 h in the presence of catalytic (1−2 mg) lithium diisopropylamide.

Kinetic Methods. Eliminations in C_6D_6. In a drybox, a small sample (ca. 3 mg, 6 μmol) of crystalline **1** was placed in a dry medium-walled NMR tube that had been sealed onto a female 14/20 joint. The tube was affixed to a stopcock adaptor, removed from the drybox, and attached to a vacuum line. The line was purged with the atmosphere from the tube, and the crystals were exposed to dynamic vacuum for several minutes to remove any volatiles. C_6D_6 (ca. 0.5 mL) was condensed into the tube using liquid nitrogen, and a known amount of hexamethyldisiloxane, $((CH_3)_3Si)_2O$, was transferred in using a known volume bulb. The tube was then flame sealed under vacuum. After an initial ^{1}H NMR spectrum was recorded, the tube was immersed in a thermostated oil bath at a specified temperature, withdrawn periodically, and quickly cooled to room temperature. The reactions were followed by ^{1}H NMR spectroscopy of the room-temperature samples. The individual Tp^{Me_2}-methine signals were integrated against the sum. These data were fitted to equations for consecutive, irreversible first-order reactions using the program EXCEL.

Eliminations in Toluene-d_8. In a drybox, a small sample (ca. 3 mg, 6 μmol) of **1** was weighed into an NMR tube with a Teflon stopcock (Young tube), a capillary with ferrocene in C_6D_6 was added as standard, and the platinum complex was dissolved in tol-d_8. The sample was degassed by several freeze−pump−thaw cycles, refilled with nitrogen, and sealed. The temperature of the NMR probe was directly measured with a thermocouple. The sample was inserted into the spectrometer and allowed to equilibrate for a couple of minutes prior to acquisition of the NMR spectra (one scan per spectrum) in given time intervals.

Eliminations in Other Solvents. ^{1}H NMR samples were prepared and treated as described above. Integration of the $Pt(CH_3)_2$ resonance of **1** against the hexamethyldisiloxane internal standard gave kinetic data, which were fitted by linear least-squares regression of a natural log plot using the program CRICKETGRAPH.

Equilibration of $Tp^{Me_2}Pt(CH_3)_2D$ (1-d_1) and $Tp^{Me_2}Pt(CH_3)(CH_2D)H$ (1-d_1'). A ^{1}H NMR sample of $Tp^{Me_2}Pt(CH_3)_2D$ (**1-d_1**) was prepared as described above and was inserted into a warm NMR probe. The tube was allowed to reach thermal equilibrium, and spectra were recorded periodically as the reaction ran continuously to equilibrium. Reaction temperatures were determined from a thermocouple at the probe, which was calibrated by the methanol technique. As the reaction progressed, the central (i.e., non-^{195}Pt coupled) $Pt(CH_3)_2$ singlet peak diminished and was replaced by a $Pt(CH_3)$ singlet and a complex signal for the diastereotopic, deuterium-coupled $Pt(CH_2D)$ protons. Relative concentrations of **1-d_1** and **1-d_1'** were assessed by the relative normalized integrals of the representative singlets. The **1-d_1** singlet overlapped slightly with the **1-d_1'** CH_2D multiplet, and a correction was made by subtracting 2/3 the integral of the **1-d_1'** singlet from the combined integrals of the **1-d_1** singlet and the **1-d_1'** multiplet. The correction was very small through 2.0$t_{1/2}$; a clear exponential decay continued past this point, but later data were of insufficient quality to include in a kinetic fit.

Thermolysis of $Tp^{Me_2}Pt(CH_3)_2(H)$ (1) in Cyclohexane. A sample of **1** (0.015 g, 0.029 mmol) and a sealed capillary tube of C_6D_5Br were placed in a J-Young tube under nitrogen. Cyclohexane (ca. 0.7 mL) was added. The sample was frozen in liquid nitrogen and evacuated under dynamic vacuum. After an initial ^{1}H NMR spectrum was obtained, the NMR tube was placed in a mineral oil bath held at a temperature of 115 °C for 5 days. Upon cooling to room temperature, the volatile components were transferred under vacuum away from the Pt black residue to another J-Young tube containing a sealed capillary tube of C_6D_5Br to be used as an NMR lock signal. After a ^{1}H NMR spectrum was obtained of the volatile components, cyclohexene (4 μL) was added to confirm the assignment of the product as cyclohexene. A blank NMR spectrum of cyclohexane revealed no cyclohexene signals. ^{1}H NMR data of the volatile components (298 K, δ): 6.02 (t, 2H, C_6H_{10} (olefin protons)), 2.39 (m, 4H, C_6H_{10}), 2.03 (m, 4H, C_6H_{10}), 1.88 (s, 12H, C_6H_{12}).

X-ray Crystallography. Single crystals of **3** were mounted on a glass fiber after recrystallization from methylene chloride at low temperature. Diffraction data were collected on a Bruker SMART diffractometer using the ω-scan mode. Refinement was carried out with the full-matrix least-squares method based on F (NRCVAX) with anisotropic thermal parameters for all non-hydrogen atoms. Hydrogen atoms were inserted in calculated positions and refined riding the corresponding atom. Details of data collection and derived parameters are included in the Supporting Information.

Acknowledgment. This research was supported by grants from the National Science Foundation. We thank Jennifer Look and Nicole Smythe for helpful discussion and Cynthia Norris for experimental assistance.

Supporting Information Available: Table S1 and Figures S1 and S2 (PDF) and X-ray crystallographic data files (CIF) for **3**. This information is available free of charge via the Internet at http://pubs.acs.org.

JA028477T

(44) Scott, J. D.; Puddephatt, R. J. *Organometallics* **1983**, *2*, 1643.